*Biochimica et Biophysica Acta*, 339 (1974) 10–29


BBA 76565

# STRUCTURE AND MORPHOLOGY OF PHOSPHATIDYLSERINE DISPERSIONS

D. ATKINSON, H. HAUSER, G. G. SHIPLEY* and J. M. STUBBS

*Biophysics Division, Unilever Research Laboratory Colworth/Welwyn, The Frythe, Welwyn, Herts. (Great Britain)*

(Received September 18th, 1973)

## SUMMARY

1. In contrast to egg phosphatidylcholine, aqueous dispersions of phosphatidylserine exist as a single lamellar liquid crystalline phase up to a water content of approx. 75% with all the water intercalated between the bilayers. In the absence of salt the lamellae of the large multilamellar particles present in dispersions ($c$ = (g lipid)/(g lipid + g water) $> 0.2$) are corrugated, particularly the outer lamellae. In the absence of salt planar phosphatidylserine bilayers are less stable than those of neutral phosphatidylcholine.

2. At low lipid concentrations ($c < 0.05$) the structural organisation is not yet clearly defined but theoretical X-ray scattering curves calculated for model particles suggest that no extensive multilamellar packing remains.

3. Sonication of phosphatidylserine dispersions produces vesicles varying in size and surrounded by a closed, single bilayer in which the structural organisation of the fundamental lipid bilayer is maintained. In the absence of salt the average vesicle diameter is 16.5 nm (165 Å), about 7–10 nm (70–100 Å) smaller than the average diameter of phosphatidylcholine vesicles. In the presence of salt (0.1 M NaCl, 0.01 M Tris, pH 8.1) the average vesicle diameter is 25 nm (250 Å) identical with that of phosphatidylcholine vesicles.

4. Reducing the double layer repulsion by adding NaCl to unsonicated dispersions ($c \gtrsim 0.05$) leads to the extrusion of water from the interbilayer space and a reduction in the lamellar repeat distance. The multilamellar particles shrink and their lamellae become smooth, indicative of an ordering in the packing of the lamellae. In dilute unsonicated dispersions ($c \lesssim 0.05$) increasing the ionic strength increases the order and extent of the multilamellar structures. Increasing the ionic strength in sonicated dispersions containing single shelled vesicles leads to aggregation and/or coalescence producing larger single bilayer vesicles as well as multilamellar structures.

5. Time-dependent structural changes in unsonicated phosphatidylserine dispersions in salt-free water are observed which are due to the reorganization of small multilamellar regions, randomly oriented with respect to each other, into more exten-

* Present address: Biophysics Division, Department of Medicine, Boston University School of Medicine, 80 East Concord Street, Boston, Mass. 02118, U.S.A.

sive and more ordered multilamellar regions. Aggregation and/or coalescence of single bilayer vesicles occurs in sonicated phosphatidylserine dispersions. This process is temperature dependent and increases with increasing temperature. The structures present in aqueous dispersions after preparation are not in thermodynamic equilibrium.

6. Structural details derived from X-ray diffraction and electron micrographs of freeze-etched preparations of phosphatidylserine dispersions are consistent with each other. The negative-staining procedure, however, produces artifacts with dispersions of acidic phospholipids.

---

## INTRODUCTION

Although proteins play an integral role in the assembly and functioning of biological membranes [1], the use of bimolecular lipid layers as models for biological membranes continues unabated [2–9]. This is justified because the lipid bilayer has been shown to be an integral part of biological membranes [5, 8]. Phosphatidylserine bilayers present in aqueous dispersions have been used frequently as model membranes (e.g. refs 10 and 23) and in the study of lipid–protein interactions (e.g. refs 11 and 12), but yet no systematic study of their structure and morphology has been reported. Here we compare structural and morphological features of aqueous phosphatidylserine dispersions with the more extensively studied phosphatidylcholine (lecithin) dispersions [9, 13–16].

## MATERIALS AND METHODS

Hen egg phosphatidylcholine and the monosodium salt of ox brain phosphatidylserine were purchased from Lipid Products (South Nutfield, Surrey, U.K.) and purified as described earlier [17]. The preparation of samples for X-ray diffraction and electron microscopy was also described in ref. 17. Aliquots (3–4 ml) of the dispersions were sonicated for 20 min under conditions (cf. ref. 18) which did not produce more than 5% degradation (mainly lysophosphatidylserine and fatty acid). More concentrated lipid dispersions ($c$ = (g lipid)/(g lipid+g water) $\geqslant$ 0.2) for X-ray analysis were homogenized in sealed sample tubes, with a narrow constriction in the middle of the tube, by centrifuging them back and forth through the narrow part of the tube. All experiments were carried out at room temperature.

X-ray scattering measurements on dilute dispersions were made using a Kratky slit-collimated camera [9] and the scattering curves were corrected for the influence of the geometry of the collimation system using the method of Taylor and Schmidt [19]. X-ray diffraction measurements at high lipid concentrations were made using a slit-collimated Rigaku-Denki low-angle camera and photographic recording methods. Methods of electron microscopy have been described elsewhere [20].

## RESULTS

### *X-ray diffraction/scattering*

Unsonicated aqueous dispersions of phosphatidylserine exhibit a lamellar phase over a wide concentration range. This behaviour is illustrated in Fig. 1 which

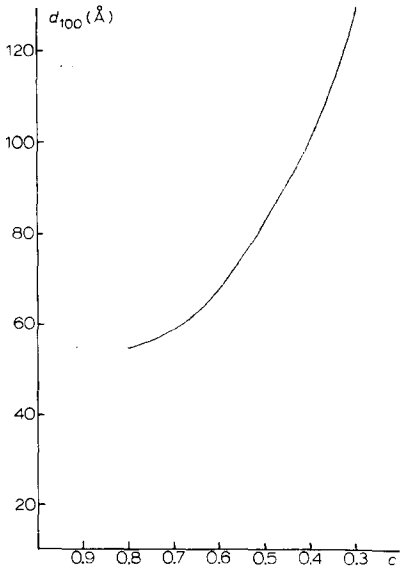


Fig. 1. X-ray diffraction spacings ($d_{100}$) from phosphatidylserine–water mixtures as a function of the lipid concentration $c$.

shows the lamellar (lipid+water) repeat distance $d$ as a function of lipid concentration $c$ (g lipid)/(g lipid+g water). At water contents $> 75\%$ ($c < 0.25$) this multilamellar, one-dimensional order no longer exists and the sharp diffraction pattern is replaced by broad diffuse scattering in the region $0.5 < h < 1.5$ nm$^{-1}$ where $h = 4\pi \sin\theta/\lambda$. Typical X-ray scattering patterns of dilute, unsonicated dispersions of phosphatidylserine ($c = 0.025$ and 0.05) are shown in Figs 2a and 2b. Also shown (Fig. 2c) is the scattering pattern obtained from a sonicated dispersion of phosphatidylserine ($c = 0.05$). A feature common to these three scattering patterns is the broad diffuse maximum in the region $0.5 < h < 1.5$ nm$^{-1}$.

For comparison the X-ray diffraction pattern obtained from a dilute, unsonicated dispersion of egg yolk phosphatidylcholine is shown in Fig. 2d. The sharp diffraction lines at 6.6 nm (66 Å) and 3.3 nm (33 Å) are the first and second order diffractions from the maximally hydrated multilamellar structure of egg yolk phosphatidylcholine and are identical to those obtained at higher lipid concentrations [9, 21, 22]. On sonication of the dispersion, the sharp diffraction lines loose intensity and gradually (with increasing sonication time and/or intensity) broaden to a diffuse scattering maximum (Fig. 2e), which is in the same region as those shown in Figs 2a–c. Inspection of the scattering curves in Fig. 2 shows that the X-ray scattering from sonicated lipid dispersions and from unsonicated phosphatidylserine (Fig. 2a) are almost identical particularly in the region of the broad scattering maximum.

In the presence of 0.5 M NaCl precipitation occurred from both sonicated and unsonicated dispersions of phosphatidylserine ($c = 0.05$). This precipitate was centrifuged at 2000 rev./min and the X-ray diffraction from the resulting pellets recorded. For both types of initial dispersion the X-ray diffraction patterns thus obtained showed sharp diffraction lines typical of a multilamellar organization with a lamellar

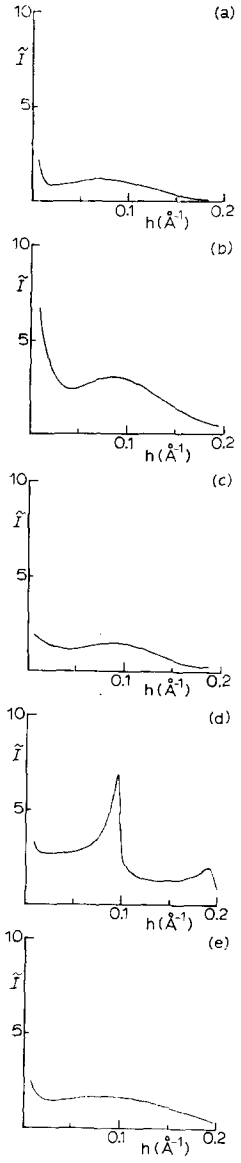


Fig. 2. X-ray scattering curves from dispersions of phosphatidylserine and phosphatidylcholine: (a) phosphatidylserine ($c = 0.025$), unsonicated; (b) phosphatidylserine ($c = 0.050$), unsonicated; (c) phosphatidylserine ($c = 0.050$), sonicated; (d) phosphatidylcholine ($c = 0.050$), unsonicated; (e) single-shelled egg phosphatidylcholine vesicles ($c = 0.050$), sonicated and fractionated by gel filtration on Sepharose 4B [18, 20]. Correcting the scattering curves for the effect of the collimation system did not significantly alter the shape of the curves. Therefore $\tilde{I}$ in Fig. 2 is the experimental scattering intensity; $h = (4\pi \sin \Theta)/\lambda$ where $2\Theta$ is the scattering angle and $\lambda$ the wavelength.

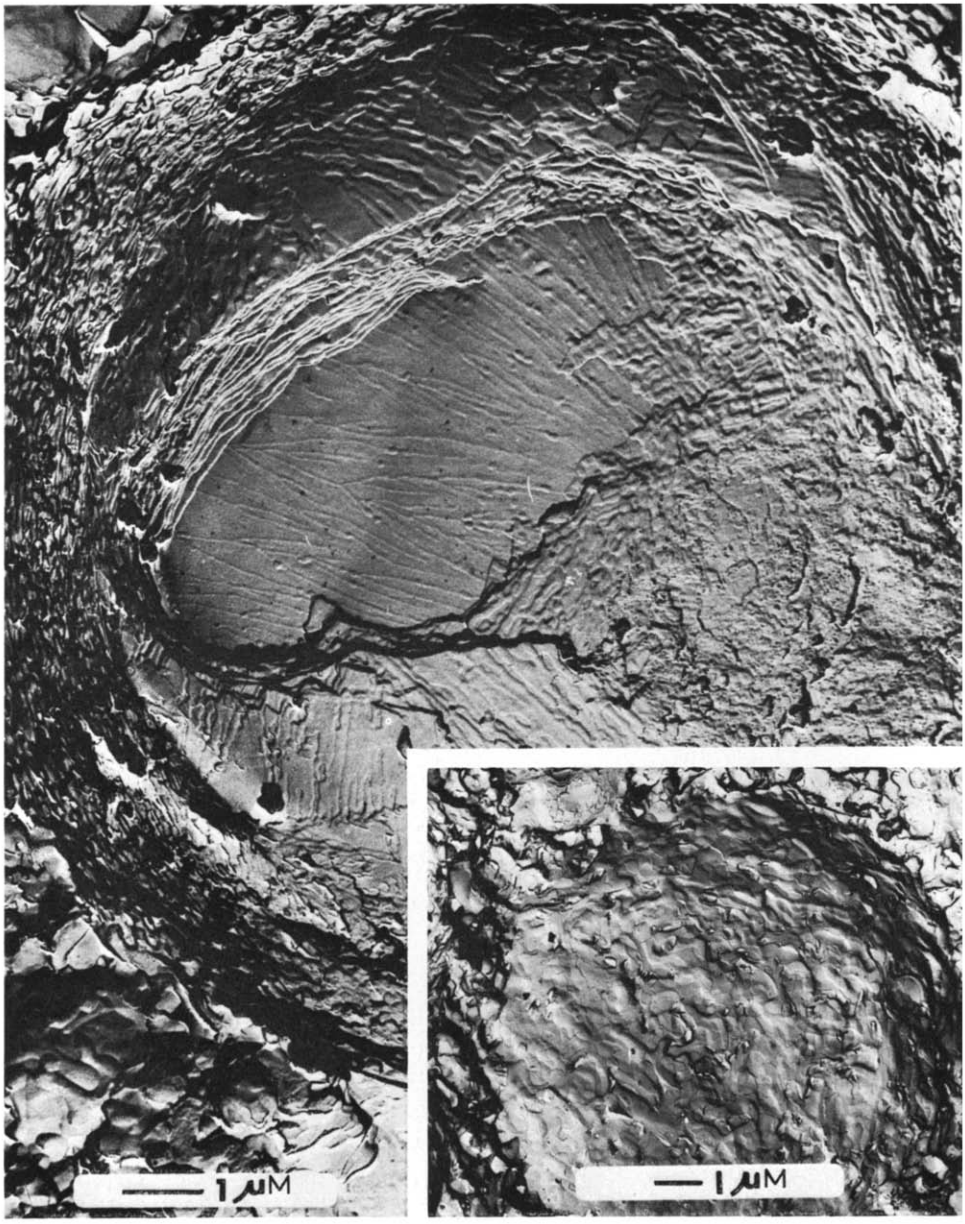


Fig. 3a

Fig. 3. Electron micrographs of (a) a freeze-etched preparation of an unsonicated phosphatidylserine dispersion ($c = 0.20$) in water. The inset is a surface view of a bilayer located in the outer region of the particle. (b) Freeze-fractured preparation of an unsonicated phosphatidylserine dispersion ($c = 0.01$) in water. The inset is a cross section of one of the less frequent multilamellar particles. (c) A negatively stained preparation of an unsonicated phosphatidylserine dispersion ($c = 0.20$) in water. The higher magnification of the inset clearly shows the presence of single bilayer vesicles containing the negative stain. (d) An unsonicated phosphatidylserine dispersion ($c = 0.01$) in water.

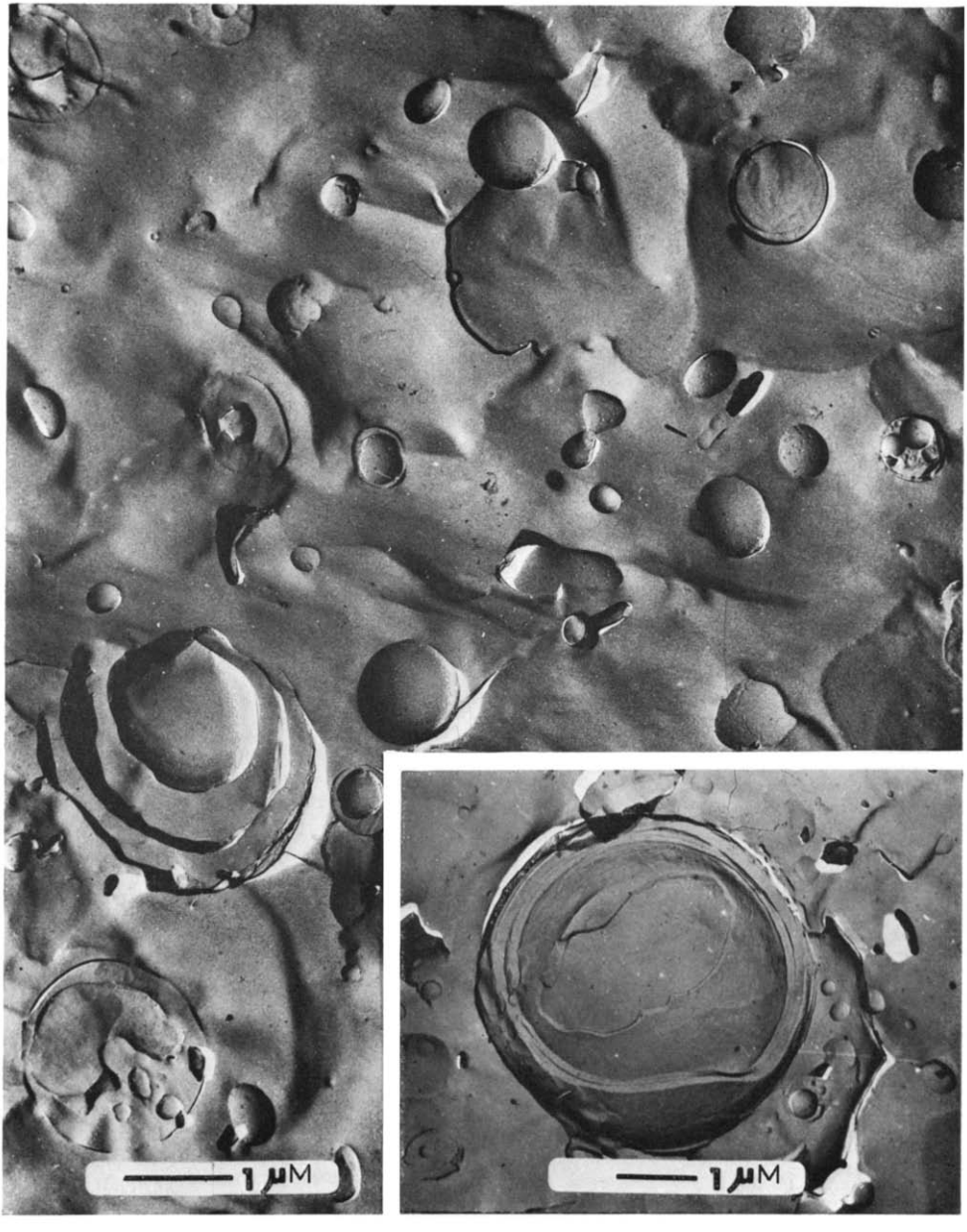


Fig. 3b

The concentrations in (c) and (d) represent the original concentrations before dilution with the negative stain. (e) A freeze-etched preparation of an unsonicated phosphatidylserine dispersion ($c = 0.2$) in buffer (0.1 M NaCl, 0.01 M Tris, pH 8.1). The plane of fracture changes frequently between adjacent bilayers indicated by the dark lines on the surface (arrow). Negatively stained samples were prepared by rinsing the phospholipid dispersion with 2 % solutions of potassium phosphotungstate, pH 7.

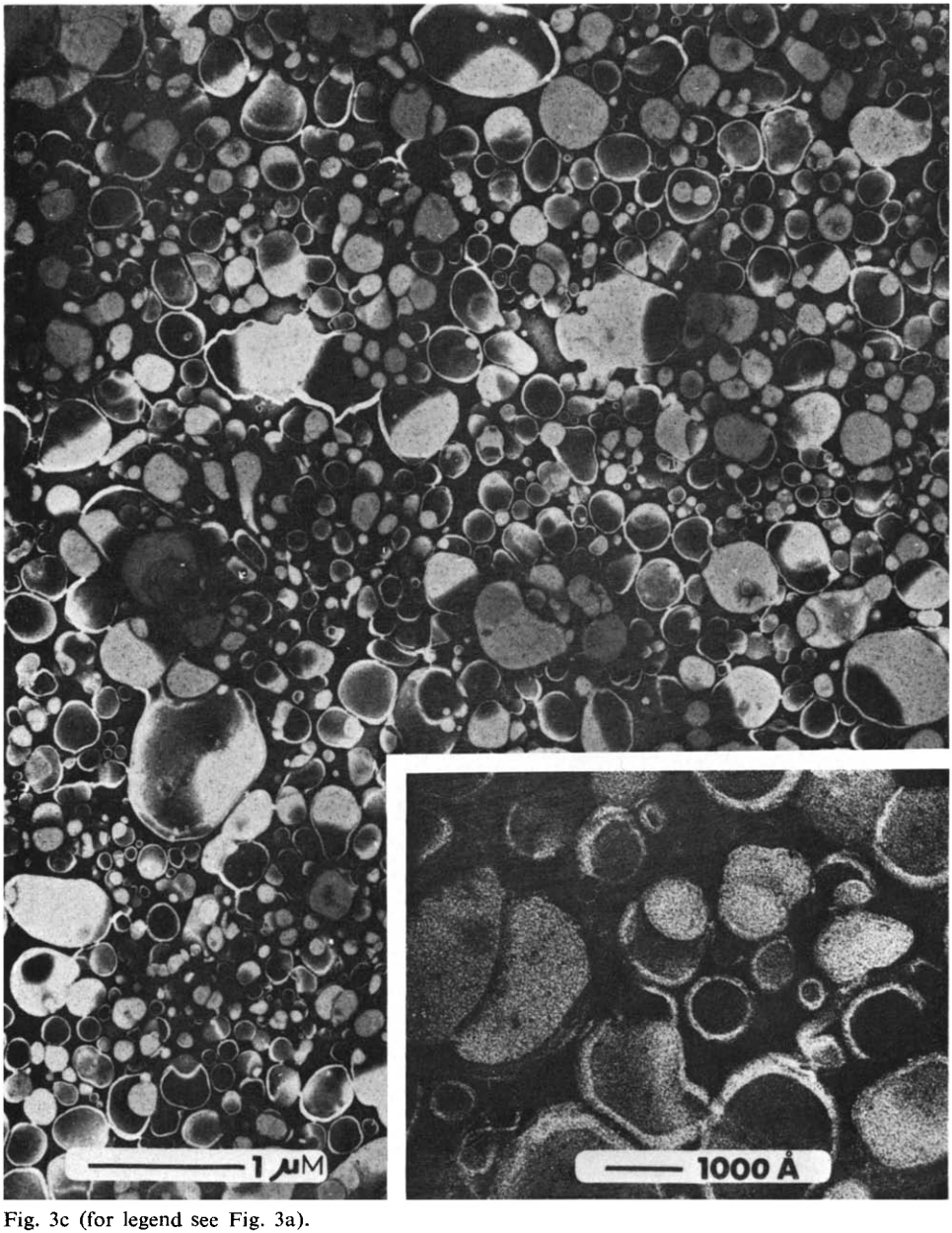


Fig. 3c (for legend see Fig. 3a).

repeat distance of 6.0 nm (60 Å). In some cases weaker diffraction lines from multilamellar structures of different dimensions were observed in addition to the principal 6.0 nm (60 Å) diffraction.

*Electron microscopy*

*Unsonicated dispersions in the absence of salt.* Fig. 3a shows an electron micro-

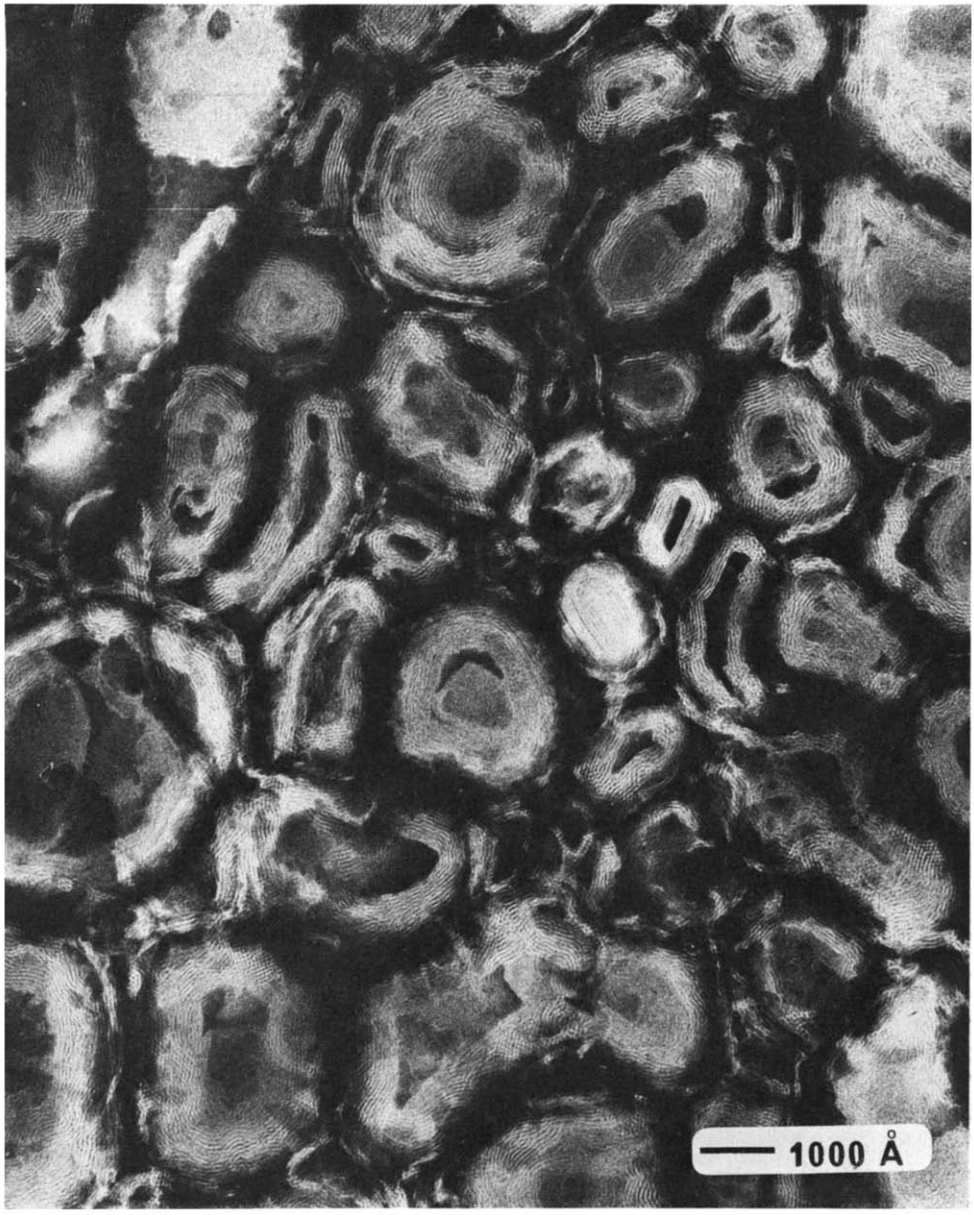


Fig. 3d (for legend see Fig. 3a).

graph of a freeze-etched preparation of an unsonicated dispersion of phosphatidylserine in water ($c = 0.20$). Stacks of bilayers reminiscent of unsonicated phosphatidylcholine dispersions [9] are observed but in contrast to the smooth appearance of phosphatidylcholine bilayers the phosphatidylserine bilayers, particularly on the outside of the large lipid particles (5–15 $\mu$m diameter), reproducibly appeared perturbed and convoluted (see inset of Fig. 3a). Cross-sectional views of the particles reveal that the

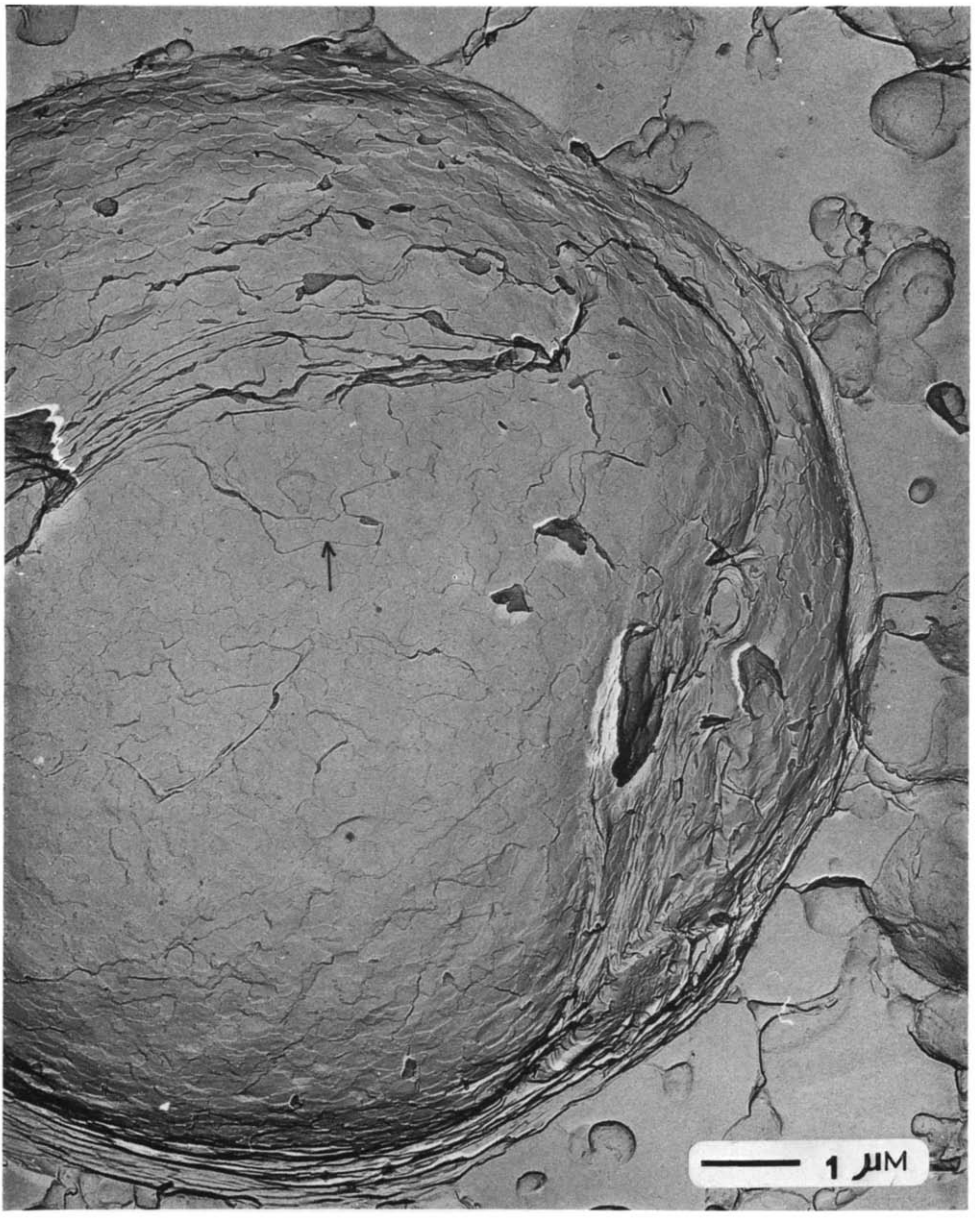


Fig. 3e (for legend see Fig. 3a).

bilayers become progressively smoother towards the center of the particles.

Fig. 3b is an electron micrograph of a freeze-fractured preparation of a dilute, unsonicated phosphatidylserine dispersion ($c = 0.01$) in water. The spherical particles observed range in size from about 0.1–15 $\mu$m, the size distribution showing that 90% of the particles have a diameter between 0.1–2 $\mu$m. There are also a few large, multilamellar particles present (Fig. 3b, inset), but less than 1% of the particles present are

of this type. Cross-sectional views reveal that the interior of most particles contains solvent or smaller particles which also seem to lack the multilamellar structure typical for egg phosphatidylcholine particles. Figs 3c and 3d are electron micrographs of negatively stained preparations of the same phosphatidylserine dispersions which were used for the freeze-etched/fractured preparations described in Figs 3a and 3b, respectively. The structures observed after negative staining are dominated by artefacts (see discussion). The particles in Fig. 3c are considerably smaller than those shown in Fig. 3a. The particle size distribution spans from 20–30 nm (200–300 Å) to about 1 $\mu$m. Most of the smaller particles some of which appear to be surrounded by a single bilayer contain negative stain in their internal cavity. The particles shown in Fig. 3d differ from those of Fig. 3b in their multilamellar order although the particle diameters are similar in both preparations.

There is evidence of time dependent structural changes in unsonicated phosphatidylserine dispersions in the absence of salt. The outer surfaces of the lamellae become progressively smoother when stored at 4 °C under $N_2$, thus preventing any significant chemical degradation. This observation of an increased long-range order is consistent with X-ray diffraction studies carried out on concentrated phosphatidylserine dispersions (up to $c \approx 0.6$) as a function of storage time. The position of the diffraction peak characteristic of the lamellar repeat distance $d$ did not change, however the diffraction maxima became sharper as time progressed.

*Unsonicated dispersions in the presence of salt.* Addition of salt (0.1 M NaCl, 0.01 M Tris, pH 8.1) to unsonicated phosphatidylserine dispersions (c = 0.2) caused smoothening of the lamellae (Fig. 3e). The particles shrank consistent with a decrease of the X-ray long spacing and the specific viscosity decreased compared with phosphatidylserine dispersions of the same concentration in water. Addition of NaCl (0.1 M) to dilute dispersions ($c = 0.01$) increased the average particle size and thus the turbidity of the dispersion. Electron microscopy and X-ray diffraction indicate that larger, multilamellar particles are formed.

*Sonicated dispersions in the absence of salt.* Sonication of phosphatidylserine dispersions leads to rupture of the larger particles and the formation of small single-bilayer vesicles [23] the size of which depends on the salt content and the phospholipid concentration [24]. The diameter of the vesicles ranged from 12.5 to 25.0 nm (125 to 250 Å) with an average of 16.5 $\pm$ 1 nm (165 $\pm$ 10 Å) (Fig. 4a), a value considerably smaller than the average diameter of 23–25 nm (230–250 Å) obtained with single-bilayer egg phosphatidylcholine vesicles [15]. Negatively stained preparations of the same phosphatidylserine dispersion gave inconsistent results. In some cases the single-bilayer vesicles appeared to have aggregated and/or coalesced to larger multilamellar particles containing up to approximately twelve bilayers (see Fig. 4b), whilst in others (Fig. 4c) they were largely preserved. The peak of the particle size distribution derived from Fig. 4c was shifted slightly to higher values compared with that derived from Fig. 4a. As with single-bilayer phosphatidylcholine vesicles there was, in general, no negative stain in the internal compartment [23].

Single-bilayer phosphatidylserine vesicles were not completely stable at room temperature and aggregation and/or coalescence to larger structures was observed. The stability of the vesicles was temperature dependent. Bilayer aggregation/fusion, monitored by gel filtration on Sepharose 4B, was negligible at 4 °C and increased with increasing temperature (cf. ref. 25).

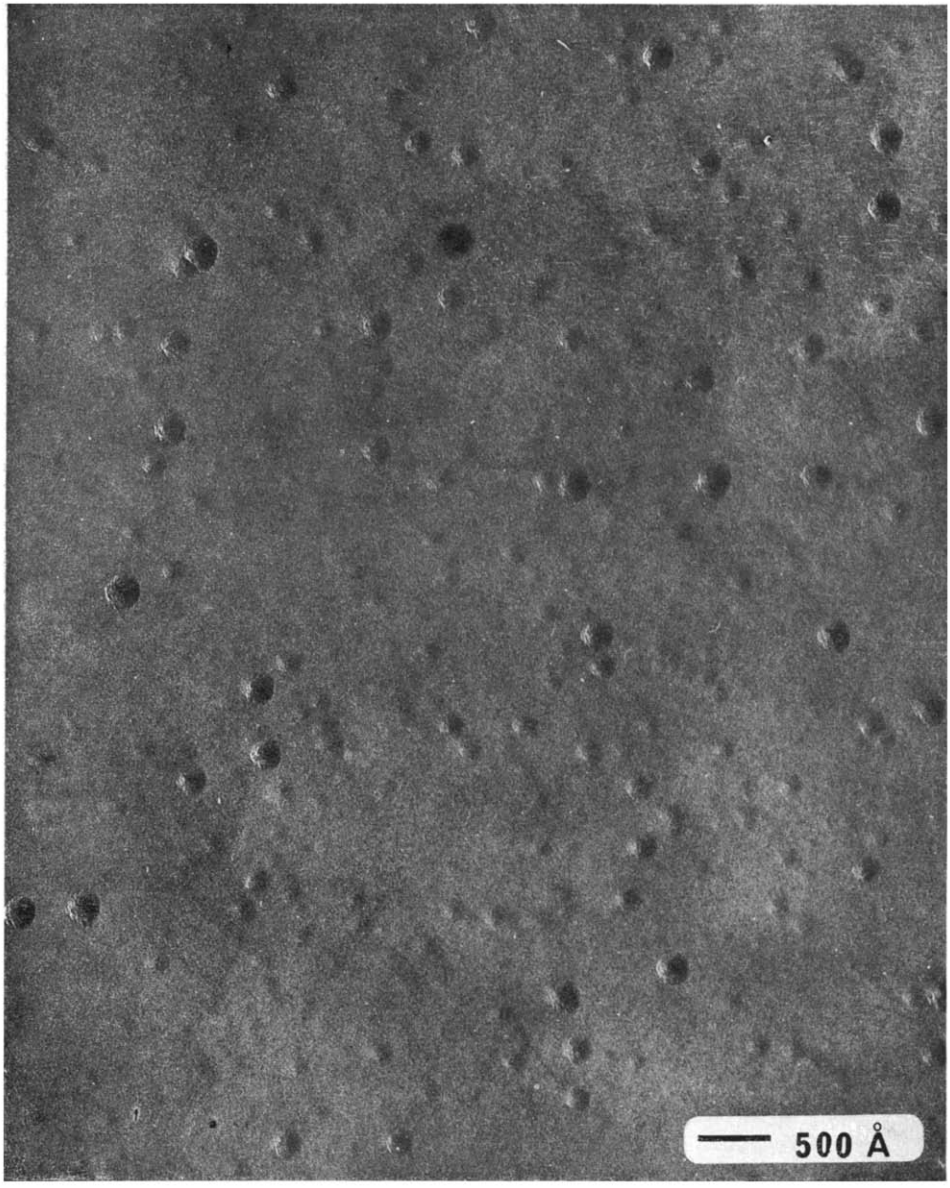


Fig. 4a

Fig. 4. Electron micrographs of (a) a freeze-etched preparation of a phosphatidylserine dispersion ($c$ = 0.01) in water, sonicated for 20 min. (b) and (c) Negatively stained samples of the same phosphatidylserine dispersion. (d) A freeze-etched preparation of a phosphatidylserine dispersion ($c$ = 0.01) in 0.1 M NaCl, 0.01 M Tris, pH 8.1, 0.02 % $NaN_3$, sonicated for 20 min.

*Sonicated dispersions in the presence of salt.* Sonication of a phosphatidylserine dispersion ($c$ = 0.01) in 0.1 M NaCl, 0.01 M Tris, pH 8.1, produced larger vesicles with diameters ranging between 20–60 nm (200–600 Å) (Fig. 4d). Particle size anal-

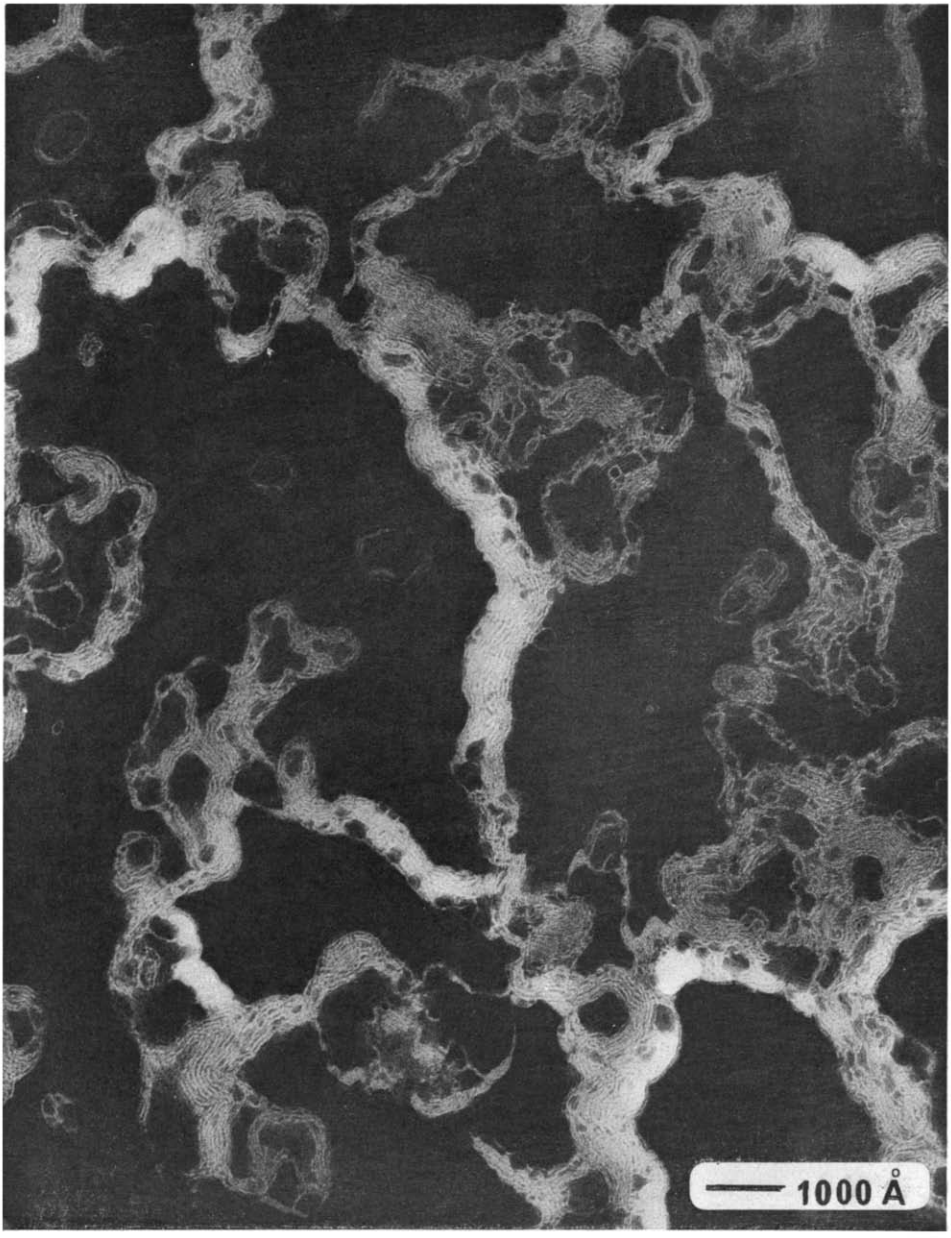


Fig. 4b

ysis of Fig. 4d gave two peaks, one centered at a diameter of 25 nm (250 Å) and the other at about 45 nm (450 Å). The size of the smaller vesicles is similar to that of sonicated phosphatidylcholine [20]. The larger vesicles probably result from the aggregation and/or coalescence of 2–4 small single-bilayer vesicles. This aggregation process was enhanced as the salt concentration increased. In 0.5 M NaCl particles,

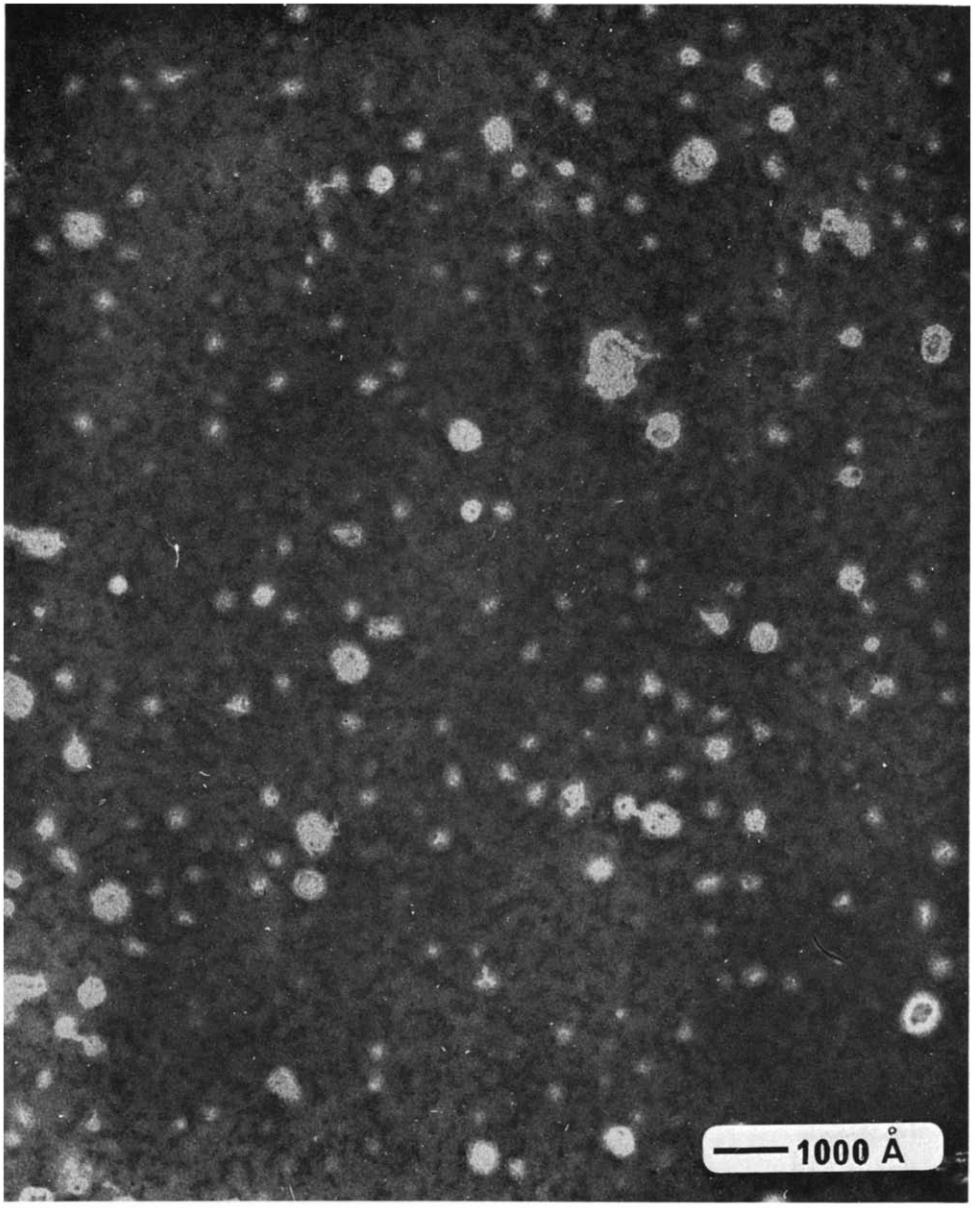


Fig. 4c (for legend see Fig. 4a).

mostly multilamellar, were observed ranging in diameter from 15 nm (150 Å) to several $\mu$m. This is consistent with X-ray diffraction data described earlier.

*Interpretation of X-ray scattering and diffraction*

The theoretical X-ray scattering has been calculated for spherical particles with increasing number of bilayers. Cross sections of the radial electron density pro-

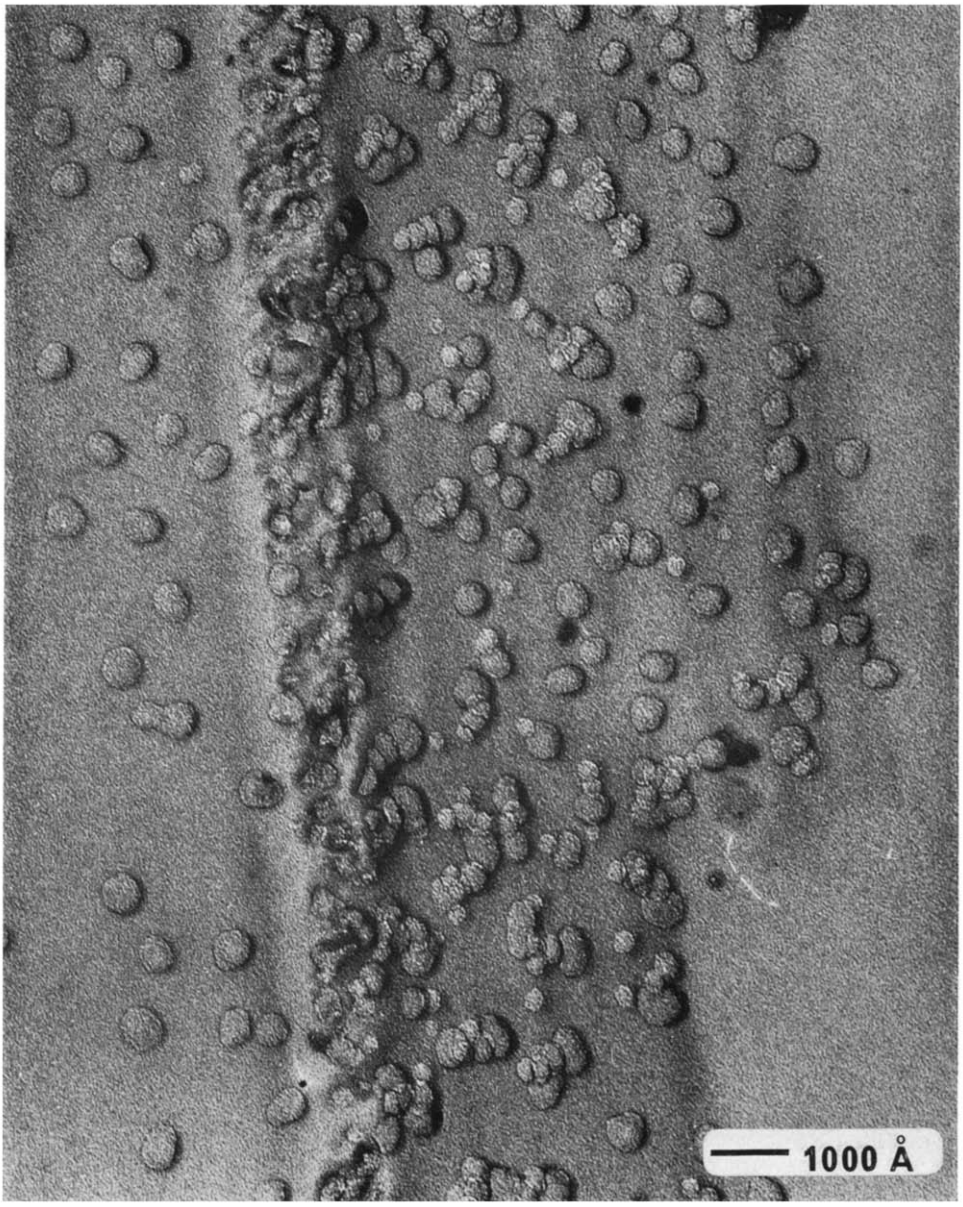


Fig. 4d (for legend see Fig. 4a.)

file of a single-bilayer vesicle and a multilamellar particle are shown in Fig. 5. The theoretical scattering for these models was calculated as a function of the radii $r_{pol}$, $r_{par}$, the electron densities $\rho_{pol}$, $\rho_{par}$ and the multilamellar order $p$ using the values for the electron densities calculated by Luzzati [26]. Figs 6a and 6b show theoretical scattering functions for vesicles surrounded by a single bilayer ($p = 1$). These functions consist of the scattering of the spherical particle modulated by the transform of

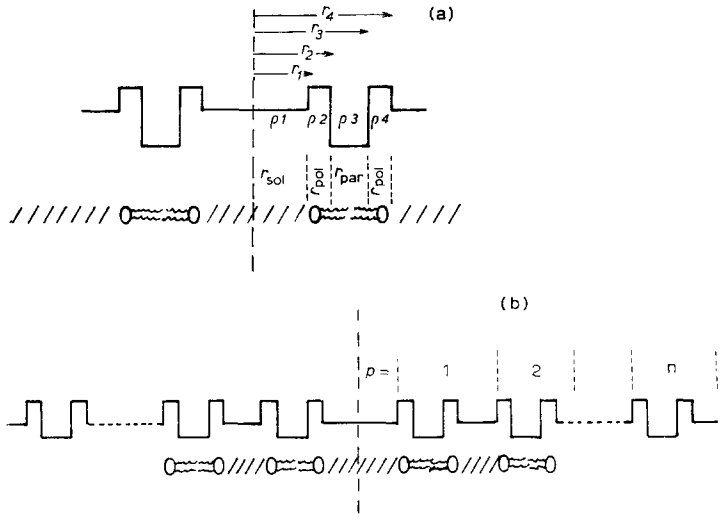


Fig. 5. Radial electron density profile of the spherical model for (a) a single bilayer vesicle; (b) a multilamellar particle.

the electron density profile of the bilayer. The curves in Fig. 6 show a series of subsidiary scattering fringes the envelope of which forms a broad diffuse maximum centered at $h \approx 1.1\ \mathrm{nm}^{-1}$. The envelopes of maxima occurring at higher values of $h$ are also indicated. The positions of the subsidiary fringes which are due to the spherical morphology (for constant values of the bilayer parameters) depend on the overall particle size. Thus for dilute dispersions containing a distribution of sizes of single shelled vesicles the observed scattering will be the sum of several scattering curves with the subsidiary maxima at different positions. The effect of "polydispersity" is illustrated in Fig. 6c by the superposition of scattering curves calculated for four particle sizes. It is clear that a smooth envelope would eventually result.

Theoretical scattering curves for particles containing 2, 3, 5, and 10 lipid–water layers surrounding a solvent core are shown in Fig. 7 for the region $0.5 < h < 1.5\ \mathrm{nm}^{-1}$. It clearly illustrates how the scattering functions of single-bilayer vesicles are modified by the addition of successive bilayer units eventually producing sharp diffraction peaks (Fig. 7d).

## DISCUSSION

With pure phosphatidylserine the increase in the lamellar repeat distance with increasing water content (Fig. 1) and the observation of a single lamellar liquid crystalline phase [27] indicates that all the water is incorporated between the lipid bilayers. This is confirmed by deuteron NMR measurements [28] which show that in phosphatidylserine–$^2H_2O$ mixtures all the water is within the bilayers over the concentration range $c = 1.0$ to 0.25 ($c = 0.25$ corresponds to 140 $^2H_2O$ molecules per lipid molecule). Similar observations were reported by Bear et al. [29] and Chapman et al. [30] who studied the swelling of beef spinal cord lipids and of a commercial sample of 1,2-dipalmitoyl-L-phosphatidylcholine, respectively.

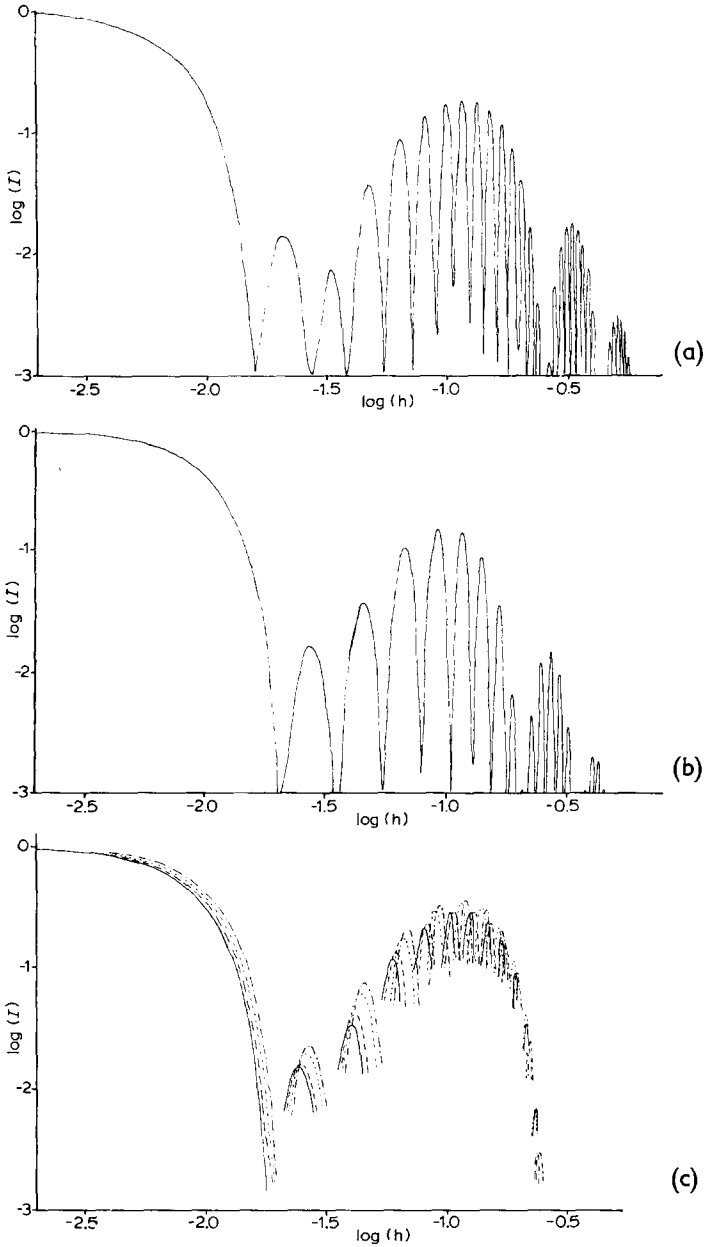


Fig. 6. Theoretical scattering curves for the single-bilayer vesicle shown in Fig. 5a:

| | | | | | |
|---|---|---|---|---|---|
| (a) $r_1 = 156$ | $\rho_1 = 0$ | | (b) $r_1 = 95$ | $\rho_1 = 0$ | |
| $r_2 = 163.5$ | $\rho_2 = 0.095$ | | $r_2 = 105$ | $\rho_2 = 0.095$ | |
| $r_3 = 192.5$ | $\rho_3 = -0.044$ | | $r_3 = 140$ | $\rho_3 = -0.044$ | |
| $r_4 = 200$ | $\rho_4 = 0.095$ | | $r_4 = 150$ | $\rho_4 = 0.095$ | |

(c) Superposition of the theoretical scattering curves of single-bilayer vesicles with radius: ———, $r = 160$; - - -, $r = 155$; · · ·, $r = 145$; - · - · - · -, $r = 140$. The radii $r$ are given in Å, the electron densities $\rho$ in electrons per Å$^3$.

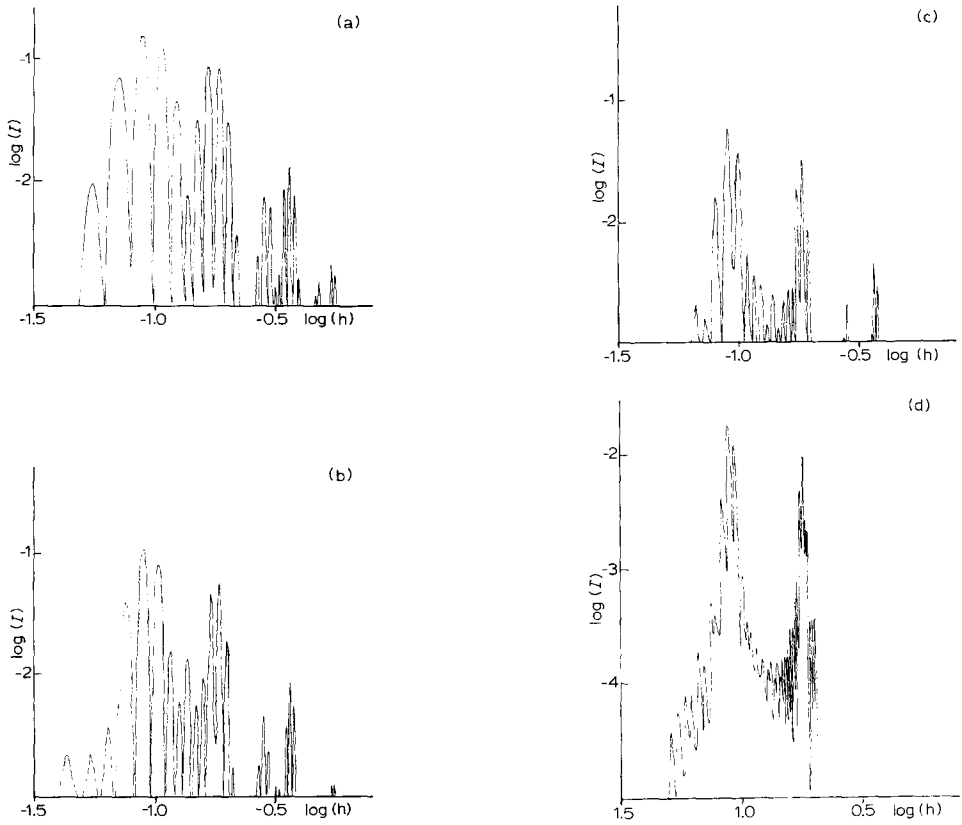


Fig. 7. Theoretical scattering curves for multilamellar particles as a function of lamellar order $p$: (a) $p = 2$; (b) $p = 3$; (c) $p = 5$; (d) $p = 10$. $r_{pol} = 7.54$ Å, $\rho_{pol} = 0.095$; $r_{par} = 29$ Å, $\rho_{par} = -0.044$. The scattering/diffraction patterns were calculated for a repeating distance of 6.6 nm (66 Å) typical for egg phosphatidylcholine at maximum hydration [24].

Pure egg phosphatidylcholine behaves differently and will incorporate water only in the range from $c = 1.0$ to 0.6 (i.e. up to about 40% water) further addition of water producing a two-phase system, a lamellar liquid crystalline phase in excess water [21, 22, 28, 31]. The ability of phosphatidylserine bilayers to incorporate large amounts of water is a consequence of the net negative charge of the phosphatidylserine molecule between pH 5–9 [32, 33] giving rise to large repulsive forces between adjacent bilayer sheets. Compared with egg phosphatidylcholine bilayers [9, 31, 34] the microscopic order of the phosphatidylserine bilayers at lipid concentrations $c \approx 0.20$ (Fig. 3a) is perturbed. The reason for this disorder is not clear. An artefact can be ruled out as a possible explanation because the perturbation seems to be localised to the outer lamellae. The conclusion is that, probably due to electrostatic repulsion, the planar bilayer of phosphatidylserine is less stable than that of neutral phosphatidylcholine (cf. ref. 35). Comparison of Figs 3a and e supports this. In the presence of ions (Fig. 3e) the lamellae are smooth as with phosphatidylcholine. This is to be expected since in the presence of counter ions screening of the net negative charge makes the phosphatidylserine head group more similar to that of phosphatidyl-

choline. This finding suggests that local changes in the ionic content can induce changes in the morphology of negatively charged bilayers. The coupling of environmental changes with changes in bilayer structure may be relevant to membrane phenomena.

At higher dilutions a two phase system, a lamellar liquid crystalline phase in excess water, is formed. The marked similarity between the X-ray scattering from unsonicated and sonicated dispersions of phosphatidylserine immediately suggests a close structural similarity between these systems. This eliminates any extensive multilamellar organization in dilute unsonicated phosphatidylserine dispersions. The presence of particles surrounded by a small but varying number of bilayers (cf. ref. 36) would account for the concentration dependence of the broad diffuse scattering observed with dilute, unsonicated phosphatidylserine dispersions (Fig. 2). Unfortunately, no conclusion regarding the number of bilayers can be derived from the electron micrograph in Fig. 3b.

The characteristic scattering curves of single-bilayer vesicles (Fig. 2) may be interpreted as the envelope of the secondary scattering fringes shown in the theoretical curves. The envelope in fact results from the one-dimensional Fourier transform of the electron density profile of the bilayer. The inhomogeneity in vesicle size as revealed by particle size analysis [15, 18, 24] would be sufficient to account for the lack of resolution of the subsidiary fringes in the experimental scattering curves (Fig. 2). These subsidiary fringes are also unresolved in the scattering curves corrected for the influence of the collimation geometry and therefore a quantitative comparison of the experimental and model scattering curves was not carried out. However, an important feature of the electron density profile of the model, necessary to produce this envelope in the scattering curve, is the region of low electron density characteristic of the hydrocarbon region of the bilayer. This feature substantiates the evidence that the fundamental bilayer structure is not changed by sonication.

The time-dependent structural changes were also observed by deuteron magnetic resonance measurements with unsonicated phosphatidylserine–$^2H_2O$ mixtures [28]. These changes were interpreted as being due to a slow reorganization and ordering of small multilamellar regions, randomly oriented with respect to each other, into more extensive multilamellar regions (1 $\mu$m in length) with strictly parallel arrays of bilayers. This interpretation is consistent with the increase in sharpness of the X-ray diffraction peak and the observation of more ordered structures in electron micrographs. A similar time dependence was observed with unsonicated phosphatidylcholine dispersions except that the time scale of the structural changes was of the order of a week rather than the month observed with phosphatidylserine. The time dependent changes were reversible and rehomogenization of the phospholipid–water mixture by centrifugation as described in Methods reversed the reorientation and ordering of the bilayers. The observation of time-dependent structural changes in phospholipid dispersions indicates that the dispersions prepared as described [17, 18] are metastable and not in thermodynamic equilibrium.

Addition of salt to concentrated, unsonicated phosphatidylserine dispersions ($c = 0.2$) reduces the double layer repulsion between adjacent bilayers. As a result of this water is extruded from the interbilayer space consistent with a decrease of the lamellar repeat distance. This also explains the observed shrinkage of the particles and the reduction in specific viscosity. Increasing the salt concentration and thus reducing the $\zeta$-potential of the bilayers also increases the order within the bilayers [24]

and induces aggregation and/or coalescence of small vesicles to larger, multilamellar structures. The observation of several lamellar spacings in addition to the principal 6.0 nm (60 Å) repeat perhaps reflects an inhomogeneous packing of bilayers possibly due to localised differences in ionic strength affecting the double layer repulsion between bilayers. High salt concentrations ($>$ 0.5 M NaCl) lead to charge neutralisation and changes in the hydration of the phospholipid polar head group which eventually cause flocculation of the phosphatidylserine–metal complex [37].

A comparison of electron micrographs of freeze-etched and negatively stained specimens (Figs 3 and 4) clearly demonstrates that the two methods of sample preparation give different structures. The results obtained with freeze-etched preparations are consistent with X-ray results indicating that the staining procedure produces artifacts. Rinsing and dilution of phosphatidylserine dispersions with 2% solutions of the stain is likely to initiate phase changes if the attainment of thermodynamic equilibrium is sufficiently rapid. The structure of the negatively stained sample in Fig. 3c (original concentration $c \approx 0.2$) is different from that of the freeze-etched preparation (Fig. 3a) and is similar to structures observed in diluted phosphatidylserine dispersions (Fig. 3b). This suggests that dilution causes the bilayers to disintegrate and the fragments then reseal to form either single bilayer vesicles or small multilamellar particles. These processes occur in the presence of the negative stain which therefore is expected to be enclosed in the internal compartments (cf. Fig. 3c).

The drying procedure involved in the preparation of negatively stained samples is also likely to induce structural changes due to the increase in ionic strength. As discussed above, such an increase in ionic strength induces the aggregation and/or coalescence of phosphatidylserine bilayers; that this occurs indeed is shown in Figs 3d and 4b. The occasional preservation of single bilayer vesicles during staining was coincidental and we could not control it. Because of these structural changes which may occur the negative staining technique is unsuitable for the structural investigation of acidic phospholipids.

ACKNOWLEDGEMENTS

Dr Shipley acknowledges the use of U.S. Public Health Service grant AM 11453-06 in the final preparation of this manuscript.

REFERENCES

1 Singer, S. J. and Nicholson, G. L. (1972) Science 175, 720–731
2 Bangham, A. D. (1968) Prog. Biophys. Mol. Biol. 18, 29–95
3 Haydon, D. A. and Hladky, S. B. (1972) Q. Rev. Biophys. 5, 187–282
4 Bangham, A. D. (1972) Annu. Rev. Biochem. 41, 753–776
5 Phillips, M. C. (1972) Prog. Surface Membrane Sci. 5, 139–221
6 Chapman, D. and Wallach, D. F. H. (1968) in Biological Membranes (Chapman, D., ed.) Vol. 1, pp. 125–202, Academic Press, London and New York
7 Shipley, G. G. (1973) in Biological Membranes (Chapman, D. and Wallach, D. F. H., eds.) Vol. 2, pp. 1–89, Academic Press, London and New York
8 Wilkins, M. H. F., Blaurock, A. E. and Engelman, D. M. (1971) Nat. New Biol. 230, 72–76
9 Chapman, D., Fluck, D. J., Penkett, S. A. and Shipley, G. G. (1968) Biochim. Biophys. Acta 163, 255–261
10 Papahadjopoulos, D., Nir, S. and Ohki, S. (1972) Biochim. Biophys. Acta 266, 561–583

11 Shipley, G. G., Leslie, R. B. and Chapman, D. (1969) Nature 222, 561–562
12 Kimelberg, H. K. and Papahadjopoulos, D. (1971) J. Biol. Chem. 246, 1142–1148
13 Huang, C. (1968) Biochemistry 8, 344–352
14 Johnson, S. M. and Bangham, A. D., Hill, M. W. and Korn, E. D. (1971) Biochim. Biophys. Acta 233, 820–826
15 Finer, E. G., Flook, A. G. and Hauser, H. (1972) Biochim. Biophys. Acta 260, 49–58
16 Hubbell, W. L. and McConnell, H. M. (1971) J. Am. Chem. Soc. 93, 314–326
17 Hauser, H., Finer, E. G. and Chapman, D. (1970) J. Mol. Biol. 53, 419–433
18 Hauser, H. (1971) Biochem. Biophys. Res. Commun. 45, 1049–1055
19 Taylor, T. R. and Schmidt, P. W. (1969) J. Appl. Cryst. 2, 143–144
20 Hauser, H. and Irons, L. (1972) Hoppe-Seyler's Z. Physiol. Chem. 353, 1579–1590
21 Reiss-Husson, F. (1967) J. Mol. Biol. 25, 363–382
22 Small, D. M. (1967) J. Lipid Res. 8, 551–557
23 Hauser, H., Phillips, M. C. and Stubbs, M. (1972) Nature 239, 342–344
24 Hauser, H. and Phillips, M. C. (1973) J. Biol. Chem. 248, 8585–8591
25 Hauser, H. and Barratt, M. D. (1973) Biochem. Biophys. Res. Commun. 53, 399–405
26 Luzzati, V. (1968) in Biological Membranes (Chapman, D., ed.) Vol. 1, pp. 71–123, Academic Press, London and New York
27 Eins, S. (1972) Chem. Phys. Lipids 8, 26–31
28 Finer, E. G. and Darke, A. (1973) Chem. Phys. Lipids 11, in the press
29 Bear, R. S., Palmer, K. J. and Schmitt, F. O. (1941) J. Cell. Comp. Physiol. 17, 355–367
30 Chapman, D., Williams, R. M. and Ladbrooke, B. D. (1967) Chem. Phys. Lipids 1, 445–475
31 Deamer, D. W., Leonard, R., Tardieu, A. and Branton, D. (1970) Biochim. Biophys. Acta 219, 47–60
32 Papahadjopoulos, D. (1968) Biochim. Biophys. Acta 163, 240-254
33 Hauser, H. and Dawson, R. M. C. (1967) Eur. J. Biochem. 1, 61–69
34 Fluck, D. J., Henson, A. F. and Chapman, D. (1969) J. Ultrastruct. Res. 29, 416–429
35 Tardieu, A., Luzzati, V. and Reman, F. C. (1973) J. Mol. Biol. 72, 711–733
36 Miyamoto, V. K. and Stoeckenius, W. (1971) J. Membrane Biol. 4, 252–269
37 Hauser, H., Phillips, M. C. and Marchbanks, R. M. (1960) Biochem. J. 120, 329–335